

PACS numbers: 42.65.Jx; 42.65.Re; 52.50.Jm
DOI: 10.1070/QE2013v043n04ABEH015110

Light bullets and supercontinuum spectrum during femtosecond pulse filamentation under conditions of anomalous group-velocity dispersion in fused silica

S.V. Chekalin, V.O. Kompanets, E.O. Smetanina, V.P. Kandidov

Abstract. **We report the results of theoretical and experimental research on spectrum transformation and spatiotemporal distribution of the femtosecond laser radiation intensity during filamentation in fused silica. The formation of light bullets with a high power density is first observed in a femtosecond laser pulse in the anomalous group velocity dispersion regime at a wavelength of 1800 nm. The minimum duration of the light bullet is about two oscillation cycles of the light field.**

Keywords: *filamentation, femtosecond pulses, anomalous dispersion, plasma channels, light bullets.*

1. Introduction

Filamentation of laser radiation represents spatiotemporal localisation of the light field, whose length in air can reach tens or hundreds of meters. The localisation of radiation in a thin filament is due to the Kerr self-focusing, which causes an increase in the intensity and, consequently, an increase in the concentration of electrons in laser plasma upon multiphoton ionisation in a strong light field of a nonlinear focus [1–3]. At equal optical powers of a focusing Kerr lens and a defocusing nonlinear plasma lens, which increases with time in the process of photoionisation, the collapsing growth of intensity in a continuous sequence of nonlinear foci forming a filament stops [4]. As a result of the dynamic balance of the Kerr and plasma nonlinearities, extended filaments with a high power density of the light field are produced. Due to the long length of the filament, high energy density and femtosecond interaction time of the light field with the medium, nonlinear-optical conversion of radiation takes place. 'Nonlinear optics of filaments' [5] covers superbroadening of the frequency-angular emission spectrum, generation of higher harmonics and THz radiation, pulse compression, filament-induced optical anisotropy, and other nonlinear optical effects accompanying the phenomenon of femtosecond filamentation.

To date, most experimental and theoretical studies of the filamentation phenomenon were performed for radiation of a Ti:sapphire laser with a wavelength of $\lambda_0 = 790–810$ nm, a neodymium laser – with $\lambda_0 = 1.053$ μm, a Cr:forsterite laser – with $\lambda_0 = 1.24$ μm, for radiation of their harmonics and for a number of different wavelengths in the case of the parametric conversion. The radiation wavelengths of these sources lie in the region of normal group-velocity dispersion (GVD) of air. Normal dispersion causes pulse spreading and its splitting into subpulses during filamentation, which significantly reduces the efficiency of broadband supercontinuum generation [6, 7], the formation of extended plasma channels [8], the transport of high-density laser radiation at kilometre distances [9, 10]. Spatiotemporal compression of femtosecond radiation of a Ti:sapphire laser was observed during filamentation in air [11], in molecular gases [12] and in argon [13–16]. At present, optical parametric chirped-pulse amplifiers (OPCPAs) have been designed for the mid-IR wavelength range [17, 18], allowing one to expand the wavelength range in research on filamentation into the region of anomalous GVD of air.

Spectroscopic studies of filamentation on extended paths in air are associated with great difficulties. However, the scenario of femtosecond laser radiation filamentation is determined by a combination of factors, such as the Kerr self-focusing and self-modulation, the light field intensity limitation and defocusing in the laser plasma and, finally, the wave diffraction and dispersion processes in the medium. Similarity criteria in the initial stage of filamentation (before the laser plasma formation) are the diffraction length and the ratio of the peak power P to the critical self-focusing power P_{cr}. Scaling the experiment on the basis of similarity criteria opens up wide possibilities for laboratory investigation of the filamentation phenomenon. A detailed study of femtosecond laser pulse filamentation in a condensed medium in a wide spectral range, which includes the region of anomalous GVD, allows one to establish the general peculiarities of this phenomenon independently of a particular medium.

Such opportunities are exhibited by a broadband femtosecond laser complex of the Centre of Collective Using 'Optical and Spectral Investigations' at the Institute of Spectroscopy, RAS [19] which allows one to carry out research in the wavelength range from UV to near IR. With this system, a series of experiments have been performed.

Conical emission (CE) has been compared for a femtosecond laser pulse focused in the volume of a glass by a lens and an axicon. As a result, it has been found that the positioning of microfilaments arising in the glass has a significantly higher reproducibility from pulse to pulse in the case of the axicon. Dark rings observed visually in the CE structure have been associated with the interference of coherent radiation sources of supercontinuum (SC) of the main and re-focused filaments

S.V. Chekalin, V.O. Kompanets Institute of Spectroscopy, Russian Academy of Sciences, ul. Fizicheskaya 5, 142190 Troitsk, Moscow, Russia; e-mail: chekalin@isan.troitsk.ru, kompanetsvo@isan.troitsk.ru; **E.O. Smetanina, V.P. Kandidov** Department of Physics, M.V. Lomonosov Moscow State University, Vorob'evy gory, 119991 Moscow, Russia; e-mail: smetanina@physics.msu.ru; kandidov@physics.msu.ru

Received 24 December 2012; revision received 4 February 2013
Kvantovaya Elektronika **43** (4) 326–331 (2013)
Translated by I.A. Ulitkin

[20]. The frequency-angular distribution of the CE in fused silica has been measured with a fibre spectrometer and the formation of a set of discrete rings from an angle continuous CE spectrum has been observed for the first time during filamentation of femtosecond, transform-limited, collimated radiation at a wavelength of 800 nm in silica. The formation of discrete rings is explained using a simple interference CE formation model, according to which its frequency-angular spectrum is the result of interference of radiation of a broadband point source moving in the filament [21, 22]. An original scheme for CE observation with a fused silica wedge has been proposed, which has made it possible to study the transformation of the angular-frequency spectrum by varying the length of the filament at constant pulse parameters. The appearance of a fine CE structure has been observed with increasing filament length, which is interpreted as the result of interference of radiation from several subpulses (into which the pulse splits in the filament under conditions of normal GVD) moving with different group velocities [23]. Conical emission has been studied during filamentation of femtosecond pulses at different GVD in the wavelength range 400–2300 nm.

To study the interference effects during the CE formation, use is made of a scheme with wedge-shaped fused silica samples, supplemented with a scheme measuring the intensity distribution of CE in the divergence angle – wavelength plane. We found [24] that the interference effects in the emission of the SC and GVD of the femtosecond pulse influence significantly the frequency-angular CE spectrum. We also studied experimentally and analytically the formation of the SC spectrum during filamentation in fused silica under conditions of zero and anomalous GVD [25, 26]. We analysed numerically the effect of the multiphoton order of the ionisation process on the anti-Stokes broadening of the SC spectrum for media with the model parameters. We found that with increasing centre wavelength from 1300 to 2300 nm the spectrum of the anti-Stokes SC wing narrows down, shifting to the blue. All experimental results were qualitatively confirmed by numerical simulations. It was shown that the mathematical model of femtosecond laser radiation filamentation used in the numerical simulation, and the interference pattern of the CE used in analytical calculations [22] adequately reproduce the observed behaviour and confirm the coherence of the SC and the CE.

In this paper we investigate the transformation of the spatiotemporal localisation of laser radiation and a frequency-angular SC spectrum during filamentation of femtosecond pulses in fused silica under conditions of anomalous GVD. It is found that the formation of light bullets is directly associated with superbroadening of the frequency-angular spectrum, which is due to the strong self-phase modulation of the light field in space and time.

2. Experiment

The SC generation during filamentation of femtosecond laser pulses of different wavelengths in fused silica was studied experimentally using a femtosecond laser complex of the Centre of Collective Using at the Institute of Spectroscopy. The experimental setup is shown in Fig. 1. The setup comprised a source of femtosecond pulses based on a tunable optical parametric amplifier TOPAS, combined with a Spitfire Pro regenerative amplifier. Pulses from a Tsunami femtosecond Ti:sapphire laser pumped by a Millenia Vs solid-state laser were fed to the regenerative amplifier pumped by an Empower 30 solid-state laser. Femtosecond laser pulses from the amplifier output were focused by a thin quartz lens with a focal length of 50 cm to the front face of the sample. At a wavelength of 1800 nm, the pulse full width at half maximum was 50 fs, the beam diameter at the waist was equal to ~100 μm, and the energy was varied from 1 to 10 μJ. The recombination radiation of the laser plasma filament and CE, scattered in the sample, was recorded through its side face by a Canon EOS 450 digital camera. It made it possible to determine the length and location of the plasma channels and to estimate the concentration of electrons in them by the brightness of the filament, thereby obtaining information about the localisation of the regions of most high intensity of the light field in the filament and, therefore, the regions of generation of SC emission.

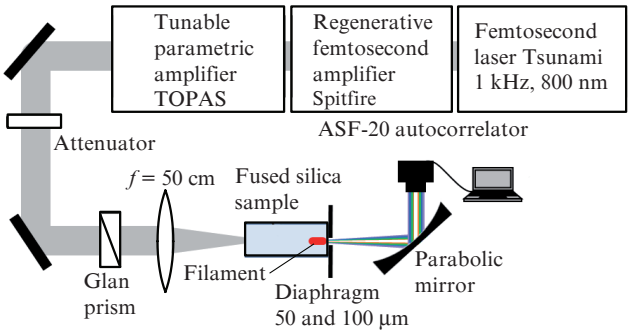

Figure 1. Experimental setup.

To measure the frequency-angular CE spectrum in the divergence angle–wavelength plane, we used an achromatic lens with a focal length of 5 cm and a Solar-Tii MS2004 monochromator, whose entrance slit is located in the focal plane of the lens. Thus, the lens performed the Fourier transform of radiation in space, and the dispersion grating of the monochromator performed the Fourier transform of radiation in time. The resulting distribution of the intensity of the spectral components of radiation $S_{\text{exp}}(\theta,\lambda)$ was recorded with a Videoskan-285-USB CCD-camera. In autocorrelation measurements of the duration of a light bullet, the paraxial part of the filament, where its formation took place, was separated by a diaphragm mounted at the output face of the sample and was collected by a parabolic mirror at the entrance window of the ASF-20 autocorrelator (Fig. 1).

The autocorrelation functions (ACFs) $J_{\text{corr}}^{\text{exp}}(t)$ of the light bullet, measured at a sample thickness of 2 and 1 cm are shown in Fig. 2 along with the ACFs of the input pulse (Fig. 2a) by solid curves; the dependences in Fig. 2b correspond to a light bullet, formed directly at the output face of the sample. In this case, the length of the plasma channel, and therefore, the length of the SC radiation generation region do not exceed 0.1 mm. By increasing pulse energy the light bullet is formed inside the sample. In the process of propagation to the output face the bullet becomes delocalised, and its duration increases. To this end, the light bullet is shifted toward the tail of the pulse, and a new bullet emerges at its centre near the output face of the sample [27]. When the first light bullet is overlapped by the second one, the pulse at the output of the sample has a double-humped shape, and the ACF $J_{\text{corr}}^{\text{exp}}(t)$ – a characteristic three-humped shape (Fig. 2c). Since the cross

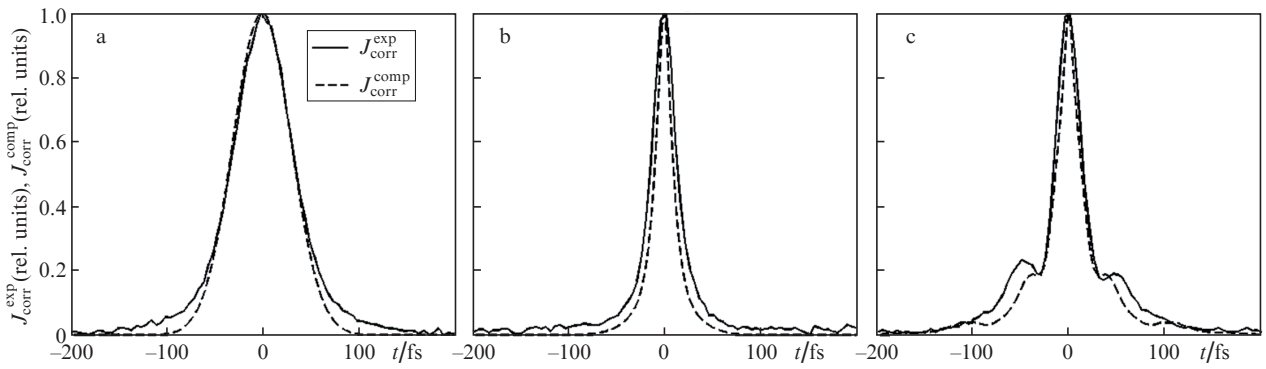

Figure 2. Measured ACFs of a light bullet during filamentation of 1800-nm, 50-fs radiation in silica [$J_{corr}^{exp}(t)$ – solid lines in all panels] and the ACFs obtained by numerical simulation [$J_{corr}^{comp}(t)$ – dashed lines in all panels] for the radiation entering the medium (the ACF width of 70 fs) (a), for a light bullet (aperture diameter of 50 μm, pulse energy of 2.7μJ, silica sample thickness of 2 cm) (b) and two light bullets (aperture diameter of 100 μm, pulse energy of 9.5 μJ, silica sample thickness of 1 cm) (c).

section of the first bullet during its propagation to the output face of the sample increases, its overlap with the second bullet is reliably recorded by using a larger diameter aperture and higher energy pulses.

3. Numerical simulation

The formation of a sequence of light bullets along the filament in fused silica was predicted in [27], based on the results of a numerical study of propagation of femtosecond laser radiation at different wavelengths. It was found that the light bullets are formed in the radiation with the centre wavelength related to the region of anomalous GVD in the medium. Bullets are formed as a result of the spatial compression of radiation in the central region of the pulse, into which (in the case of anomalous GVD) optical power is transferred from its front. According to the estimates the peak intensity of the light bullet is 5×10^{13} W cm^{-2}, its diameter is 20 μm, and the duration is about 10 fs. With increasing pulse energy, the number of light pulses in the sequence increases, and the distance between them is reduced.

The formation of light bullets in the experiment was numerically simulated using the slowly varying envelope approximation [28]. The mathematical model describes the diffraction of the pulse, its dispersion in accordance with the Sellmeier formula, self-phase modulation of the light field, the steepening of the envelope front, the Kerr nonlinearity, the plasma generation under multiphoton and avalanche ionisation in silica. The slowly evolving wave approximation [28] significantly extends the frequency range reproduced by the slowly varying envelope approximation, which is necessary for an adequate description of the broadening of the pulse spectrum and the formation of shock waves at the tail of the pulse during filamentation. Therefore, this model can be used to describe the propagation (in a medium with a cubic nonlinearity) of pulsed radiation, the spectral width of which is comparable with the carrier frequency, and duration – with one and a half cycle of optical oscillations [28, 29].

The numerical solution of the equations for the light field amplitude and the electron concentration in the laser-induced plasma made it possible to determine the spatiotemporal distribution of the intensity $I(r,t)$ in a femtosecond pulse at the output face of a silica sample in the experiment. In the autocorrelation measurements, radiation averaged over the cross section of the diaphragm was studied. Therefore, to compare the numerical results with the experimental ones we determined the effective form of the light bullet $\langle I(t)\rangle_D$, obtained by averaging over the aperture diaphragm of diameter D:

$$\langle I(t)\rangle_D = \int_0^{D/2} 8I(r,t)r\mathrm{d}r/D^2. \quad (1)$$

The analysis shows that the near-axial region of the beam in the filament, which has the smallest duration, is much smaller than the aperture of the diaphragms used in the experiment. As the diameter of the aperture increases, the contribution of the beam periphery increases, in which time compression of the pulse is small, and the duration of an effective form of the bullet increases. The ACFs $J_{corr}^{comp}(t)$, calculated from the numerically obtained effective form of the light bullet $\langle I(t)\rangle_D$ are shown in Fig. 2 by a dashed curve. One can see that for an initial pulse and a light bullet, they coincide with the measured ACFs $J_{corr}^{exp}(t)$ (Figs 2a, b). In the case of a superposition of two bullets the numerical ACF with a pronounced three-humped structure (Fig. 2c) is quite different from the measured one. This discrepancy is explained by the fact that the measurements are based on averaging over a large series of light bullets. When the pulse energies fluctuate, the distance, at which the light bullets are generated, and thus, their duration at the output of the sample change. Therefore, the tree-humped structure of the measured ACF is blurred. The effective form of the light bullet $\langle I(t)\rangle_D$, obtained numerically, and the ACF $J_{corr}^{comp}(t)$, calculated from this form are shown in Figs 3a, b, as functions of the distance z travelled in the medium. The duration and width of the ACF of the light bullet are minimal in the plane of its formation $z = 0.75$ cm (Fig. 3c). When propagating the bullet is delocalised, its duration and the ACF width increase. The formation of a sequence of light bullets reflects the periodic change in the ACF width with distance z. As can be seen from the results of numerical simulations (Fig. 3), the re-reduction of the ACF width and, therefore, the duration of radiation are possible when the second light bullet is formed at a distance of 0.9 cm. In this case the width of the measured ACF τ_{corr}^{exp} was 34 fs. The diverging lines from the regions of the formation of light bullets in a plane of the ACF transformation with distance z illustrate the appearance of a three-humped ACF when the bullets overlap each other, i.e., their simultaneous existence at a distance z in the sample (Fig. 3b). The evolution of each light bullet in a medium with anomalous GVD represents its shift to the pulse tail due to a decrease in the bullet speed

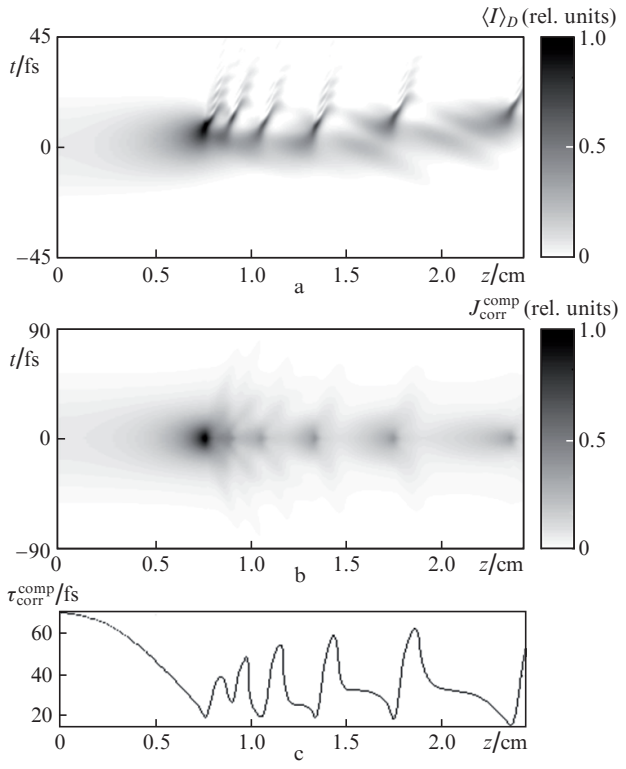

Figure 3. Numerically obtained sequence of light bullets during filamentation of 1800-nm, 50-fs, 3-μJ radiation with a peak power $4P_{cr}$ in silica: tone images of the transformation (with the distance z) of the effective form of the light bullet $\langle I(t)\rangle_D$, obtained by averaging over the aperture with a diameter $D = 50$ μm (a), the ACF of the effective form of the light bullet $J_{corr}^{comp}(t)$ (b), and change in the ACF width τ_{corr}^{comp} with distance z (c).

without a significantly change in the shape (as long as the light bullet does not leave the reservoir of energy), which is similar to the behaviour of Raman solitons in anomalous GVD fibres [30].

4. Duration of a light bullet

The effective form of the light bullet $\langle I(t)\rangle_D$, obtained numerically, is presented in normalised form in Fig. 4b at $D = 50$ μm. One can see that it is qualitatively different from the dependences that are typically used to approximate the shape of the laser pulse. In contrast to the Gaussian pulse, in the light bullet large wings are combined with a sharper leading edge and a shock front at the tail, arising due to the self-steepening effect as a result of laser-induced plasma defocusing (Fig. 4a). In this case, the temporal shape of the bullet $\langle I(t)\rangle_D$ depends on the aperture averaging. The smaller the diameter D of the selective aperture, the shorter the bullet duration $\tau_{1/2}^{comp}$, defined at the 0.5 level. The ACF $J_{corr}^{comp}(t)$, calculated from the numerically obtained effective form of the light bullet $\langle I(t)\rangle_D$ with increasing distance z travelled in the medium is shown in Fig. 3b. The minimum width of the calculated ACF τ_{corr}^{comp}, determined by the 0.5 level, at $D = 50$ μm is 19.8 fs, which corresponds to the bullet duration $\tau_{1/2}^{comp} = 10.6$ fs; when $D = 100$ μm the minimum width of the second light bullet is $\tau_{corr}^{comp} = 30$ fs, which corresponds to $\tau_{1/2}^{comp} = 14.8$ fs. Summarising the results of numerical simulations, we can show that the ratio $\tau_{1/2}^{comp}/\tau_{corr}^{comp}$ is in the range 0.44–0.7, where 0.7 corresponds to a Gaussian pulse shape at the entrance to the medium.

Using the numerical ratio between the bullet duration $\tau_{1/2}$ and the ACF width τ_{corr}, we can obtain an estimate of the duration of the experimentally recorded light bullets: $\tau_{1/2}^{exp} = 12 - 20$ fs. The minimum duration of the experimentally recorded light bullet is 11.8–13.5 fs, i.e., about two oscillation cycles of the light field for the centre wavelength of the pulse experiencing filamentation.

The formation of a light bullet with a high localisation of radiation in space and time is inextricably associated with the broadening of the frequency-angular spectrum. Figure 5 shows a tone image of the intensity of the frequency-angular spectrum components $S(\theta,\lambda)$ in a logarithmic scale. The spectrum is considered at a distance z, where the light bullet has the shortest duration. It is seen that in the vicinity of the centre wavelength the spectrum is uniformly broadened both in angle and wavelength. In addition, there is CE in the anti-Stokes wing of the SC with a low intensity of the spectral components [25, 26]. Processing of the spectrum makes it possible to evaluate whether the emission of light bullet is transform-limited. To do this, under the assumption of the phase synchronism of all the components of the spectrum we calculated the spatiotemporal intensity distribution and the corresponding effective form of the bullet $\langle I_{mod}(t)\rangle_D$ by formula (1) (Figs 4c, d). One can see that in this case the duration and the localisation region of the light field in a transform-limited light bullet are less than in a bullet formed in the filament. In the case of a transform-limited bullet $\tau_{1/2mod}^{comp} = 5.4$ fs.

5. Conclusions

During femtosecond laser radiation filamentation in fused silica under conditions of anomalous GVD, a sequence of light bullets is generated with the light field intensity of 5×10^{13} W cm^{-2}. Based on the analysis of the form of the light bullet we have found that the ratio of its duration $\tau_{1/2}^{comp}$ to the ACF width τ_{corr}^{comp} is 0.44–0.5 in the region of existence of a light bullet whose shape differs significantly from the Gaussian. To this end, we have estimated the duration of the light bullet, which at a minimum width of the measured ACF $\tau_{corr}^{exp} = 27$ fs is 11.8–13.5 fs for the selecting aperture 50 μm in diameter. In this case, complete phase synchronism of spectral SC components is not achieved in the filament and the emission of the light bullet is not transform-limited.

Acknowledgements. The study was supported by Russian Ministry of Education (Contract No. 8372), Russian Foundation for Basic Research (Grant Nos 12-02-2048-ofi_m, 11-02-00556a, 12-02-31690mol_a) and programme 'Extreme Light Fields and Their Applications' of the Presidium of RAS. V.P. Kandidov and E.O. Smetanina acknowledge the support of the President Grants for Support of the Leading Scientific Schools of the Russian Federation (No. NSh-6897.2012.2) and the Ministry of Education and Science (Agreement No. 8393).

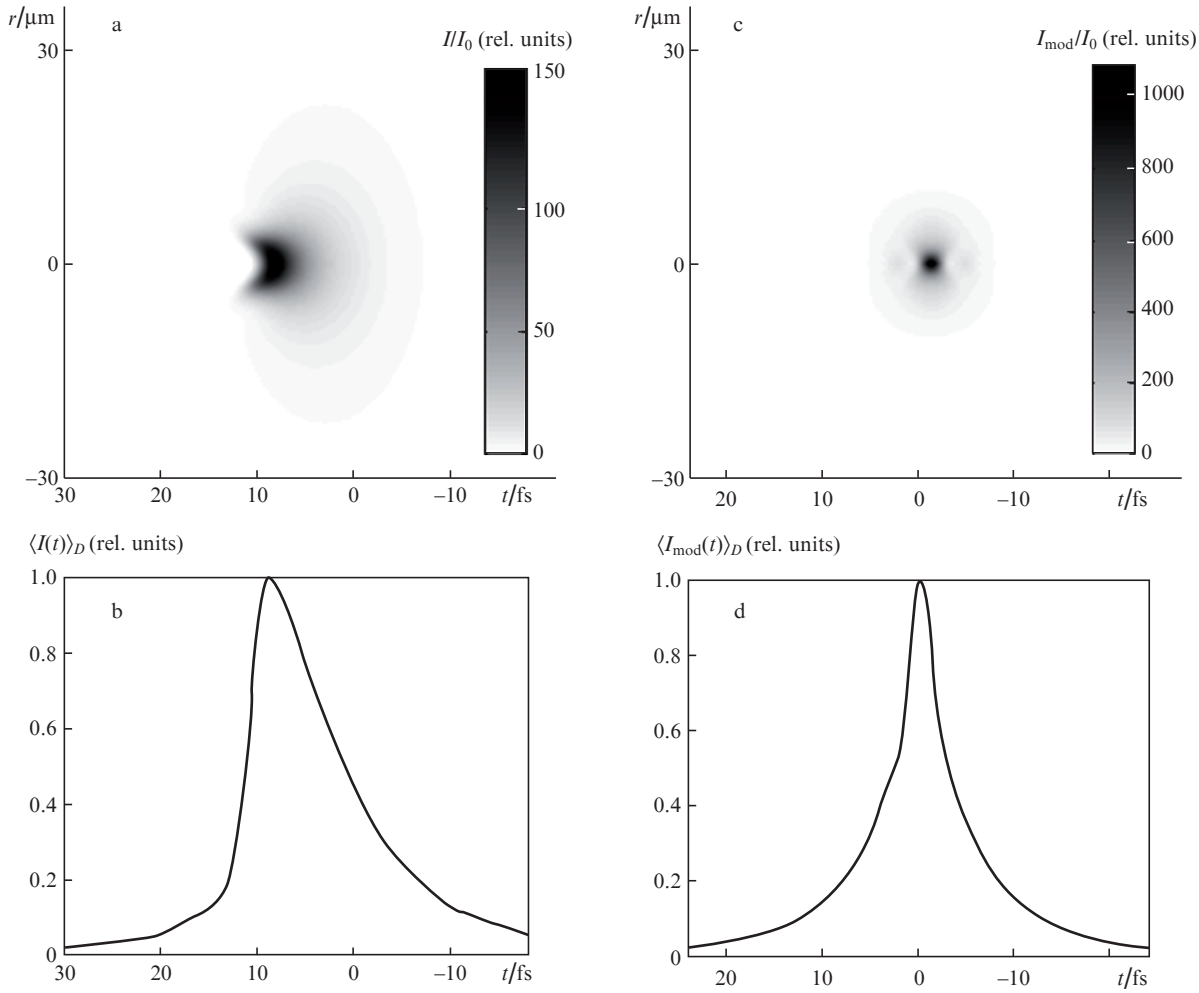

Figure 4. Spatiotemporal characteristics of the light bullet. The intensity distribution $I(r, t)$, normalised to the peak intensity I_0 (a), and the effective form $\langle I(t)\rangle_D$ (averaged over the aperture with $D = 50$ μm) (b) of the first bullet during filamentation of 1800-nm, 50-fs, 3-μJ radiation with a peak power $4P_{cr}$ in silica at a distance $z = 0.75$ cm, and the intensity distribution $I_{mod}(r, t)$ (c) and the effective form $\langle I_{mod}(t)\rangle_D$ (averaged over the aperture with $D = 50$ μm) (d) of a model light bullet with completely phased-matched components of the frequency-angular SC spectrum.

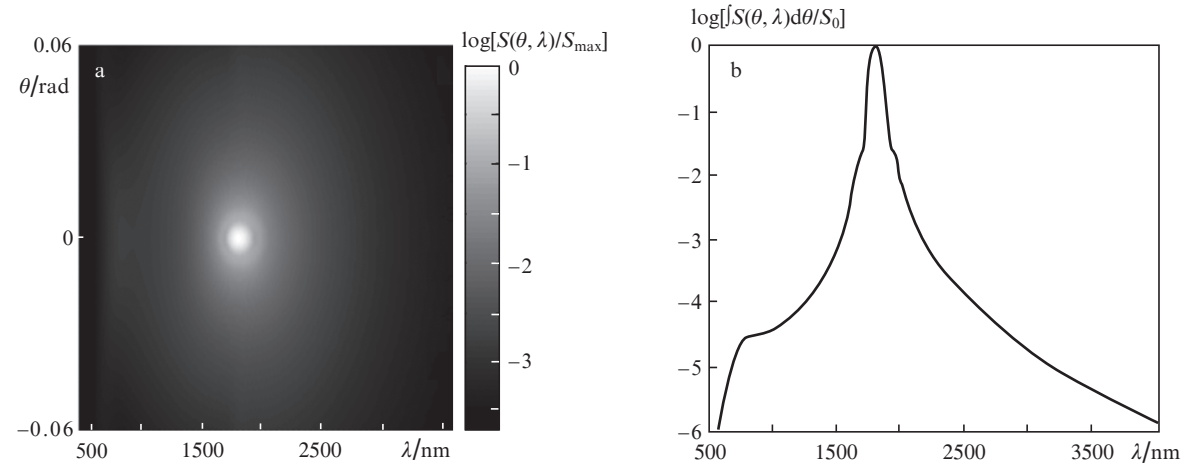

Figure 5. Spectral characteristics of the light bullet: frequency-angular SC spectrum $S(\theta, \lambda)$ (a) and frequency SC spectrum $S(\lambda) = \int S(\theta, \lambda)d\theta$ (b) of the first bullet during filamentation of 1800-nm, 50-fs, 3-μJ radiation with a peak power $4P_{cr}$ in silica at a distance $z = 0.75$ cm.

References

1. Akozbek N., Becker A., Kandidov V., Kosareva O., Schroeder H. *Can. J. Phys*., **83**, 863 (2005).
2. Couairon A., Mysyrowicz A. *Phys. Rep*., **441**, 47 (2007).
3. Kandidov V.P., Shlenov S.A., Kosareva O.G. *Kvantovaya Elektron*., **39**, 205 (2009) [*Quantum Electron*., **39**, 205 (2009)].
4. Kandidov V.P., Fedorov V.Yu., Tverskoy O.V., Kosareva O.G., Chin S.L. *Kvantovaya Elektron*., **41**, 382 (2011) [*Quantum Electron*., **41**, 382 (2011)].
5. Geints Yu.E. et al. *Nonlinear Femtosecond Atmospheric Optics* (Tomsk: Publishing House of Institute of Atmospheric Optics SB RAS, 2010) p. 212.
6. Kasparian J., Rodriguez M., Mejean G., Yu J., Salmon E., Wille H., Bourayou R., Frey S., Andre Y.-B., Mysyrowicz A., Sauerbrey R., Wolf J.-P., Woste L. *Science*, **301**, 61 (2003).
7. Golubtsov I.S., Kandidov V.P., Kosareva O.G. *Kvantovaya Elektron*., **33**, 525 (2003) [*Quantum Electron*., **33**, 525 (2003)].
8. Mechain G., D'Amico C., Andre Y.-B., Tzortzakis S., Franco M., Prade B., Mysyrowicz A., Couairon A., Salmon E., Sauerbrey R. *Opt. Commun*., **247**, 171 (2005).
9. Nuter R., Skupin S., Berge L. *Opt. Lett*., **30**, 917 (2005).
10. Kandidov V.P., Shlenov S.A. in *Glubokoe kanalirovanie i filamentatsiya moshchnogo lazernogo izlucheniya v veshchestve* (Deep Channelling and Filamentation of Intense Laser Light in a Medium) (Moscow: Interkontakt Nauka, 2009) p. 185.
11. Lange H.R., Ripoche J.F., Chiron A.A., Lamouroux B., Franco A., Prade B., Nibbering E.T.J., Mysyrowicz A., in *Proc. 11th Intern. Conf. Ultrafast Phenomena* (Berlin: Springer, 1998, p. 115).
12. Koprinkov I.G., Suda A., Wang P., Midorikawa K. *Phys. Rev. Lett*., **84**, 3847 (2000).
13. Wagner N.L., Gibson E.A., Popmintchev T., Christov I.P., Murnane M.M., Kapteyn H.C. *Phys. Rev. Lett*., **93**, 173902 (2004).
14. Stibenz G., Zhavoronkov N., Steinmeyer G. *Opt. Lett*., **31**, 274 (2006).
15. Uryupina D., Kurilova M., Mazhorova A., Panov N., Volkov R., Gorgutsa S., Kosareva O., Savel'ev A., Chin S.L. *J. Opt. Soc. Am. B*, **27**, 667 (2010).
16. Skupin S., Stibenz G., Bergé L., Lederer F., Sokollik T., Schnürer M., Zhavoronkov N., Steinmeyer G. *Phys. Rev. E*, **74**, 056604 (2006).
17. Andriukaitis G., Balčiūna T., Ališauskas S., Pugžlys A., Baltuška A., Popmintchev T., Chen M.-C., Murnane M., Kapteyn H.C. *Opt. Lett*., **36**, 2755 (2011).
18. Popmintchev T., Chen M.-C., Popmintchev D., Arpin P., Brown S., Alisauskas S., Andriukaitis G., Balciunas T., Mücke O.D., Pugzlys A., Baltuska A., Shim B., Schrauth S.E., Gaeta A.L., Hernández-García C., Plaja L., Becker A., Jaron-Becker M., Murnane M., Kapteyn H.C. *Science*, **36** (6086), 1287 (2012).
19. Chekalin S.V. *Usp. Fiz. Nau*k, **176**, 657 (2006) [*Phys. Usp*., **49**, 636 (2006)].
20. Kosareva O.G., Grigor'evskii A., Kandidov V.P., Kompanets V.O., Chekalin S.V. *Kvantovaya Elektron*., **36** (9), 821 (2006) [*Quantum Electron*., **36** (9), 821 (2006].
21. Dormidonov A.E., Kandidov V.P., Kompanets V.O., Chekalin S.V. *Kvantovaya Elektron*., **39** (7), 653 (2009) [*Quantum Electron.*, **39** (7), 653 (2009)].
22. Dormidonov A.E., Kandidov V.P. *Laser Phys.*, **19**, 1993 (2009).
23. Dormidonov A.E., Kandidov V.P., Kompanets V.O., Chekalin S.V. *Pis'ma Zh. Eksp. Teor. Fiz*., **91** (8), 405 (2010) [*JETP Lett*., **91** (8), 373 (2010)].
24. Kandidov V.P., Smetanina E.O., Dormidonov A.E., Kompanets V.O., Chekalin S.V. *Zh. Eksp. Teor. Fiz*., **140**, 484 (2011).
25. Smetanina E.O., Kompanets V.O., Chekalin S.V., Kandidov V.P. *Kvantovaya Elektron*., **42** (10), 913 (2012) [*Quantum Electron*., **42** (10), 913 (2012)].
26. Smetanina E.O., Kompanets V.O., Chekalin S.V., Kandidov V.P. *Kvantovaya Elektron*., **42** (10), 920 (2012) [*Quantum Electron*., **42** (10), 920 (2012)].
27. Smetanina E.O., Dormidonov A.E., Kandidov V.P. *Laser Phys*., **22**, 1189 (2012).
28. Brabec T., Krausz F. *Phys. Rev. Lett*., **78**, 3282 (1997).
29. Bakhtin M., Shpolyansky Yu.A. in: *Sovremennye tekhnologii (Modern Technologies)* (St. Petersburg: St. Petersburg State University, 2001) pp 12–18.
30. Agrawal G. *Nonlinear Fiber Optics* (CA, San Diego: Academic Press, 2001; Moscow: Mir, 1996).